

# Oligomeric A $\beta$ in the monkey brain impacts synaptic integrity and induces accelerated cortical aging

Danielle Beckman<sup>a</sup>, Sean Ott<sup>a</sup>, Kristine Donis-Cox<sup>a</sup>, William G. Janssen<sup>b,c</sup>, Eliza Bliss-Moreau<sup>a,d</sup>, Peter H. Rudebeck<sup>b,c</sup>, Mark G. Baxter<sup>b,c</sup>, and John H. Morrison<sup>a,e,1</sup>

<sup>a</sup>California National Primate Research Center, University of California, Davis, CA 95616; <sup>b</sup>Department of Neuroscience, Icahn School of Medicine at Mount Sinai, New York, NY 10029; <sup>c</sup>Friedman Brain Institute, Icahn School of Medicine at Mount Sinai, New York, NY 10029; <sup>d</sup>Department of Psychology, University of California, Davis, CA 95616; and <sup>e</sup>Department of Neurology, School of Medicine, University of California, Davis, CA 95616

Edited by Elizabeth A. Buffalo, University of Washington, Seattle, WA, and accepted by Editorial Board Member Tony Movshon August 8, 2019 (received for review March 11, 2019)

As the average age of the population continues to rise, the number of individuals affected with age-related cognitive decline and Alzheimer's disease (AD) has increased and is projected to cost more than \$290 billion in the United States in 2019. Despite significant investment in research over the last decades, there is no effective treatment to prevent or delay AD progression. There is a translational gap in AD research, with promising drugs based on work in rodent models failing in clinical trials. Aging is the leading risk factor for developing AD and understanding neurobiological changes that affect synaptic integrity with aging will help clarify why the aged brain is vulnerable to AD. We describe here the development of a rhesus monkey model of AD using soluble oligomers of the amyloid beta (A $\beta$ ) peptide (A $\beta$ Os). A $\beta$ Os infused into the monkey brain target a specific population of spines in the prefrontal cortex, induce neuroinflammation, and increase AD biomarkers in the cerebrospinal fluid to similar levels observed in patients with AD. Importantly, A $\beta$ Os lead to similar dendritic spine loss to that observed in normal aging in monkeys, but so far without detection of amyloid plaques or tau pathology. Understanding the basis of synaptic impairment is the most effective route to early intervention and prevention or postponement of age-related cognitive decline and transition to AD. These initial findings support the use of monkeys as a platform to understand age-related vulnerabilities of the primate brain and may help develop effective disease-modifying therapies for treatment of AD and related dementias.

Alzheimer's disease | rhesus monkey | microglia | A $\beta$ Os | synapse

Between 2010 and 2050 the US population is projected to more than double, with 88.5 million Americans age 65 y or older in 2050 (1). These numbers reinforce the importance of understanding what separates normal aging from pathological events like neurodegenerative diseases, in terms of both cognition and brain pathology. Cognitive decline and neuronal loss are not inevitable consequences of normal aging, although aging is a key risk factor for neurodegenerative processes (2, 3). For many decades it was assumed that decline in cognition with normal aging was a consequence of neuronal death, but unbiased stereological techniques have shown that there is minimal neuronal death in the cerebral cortex with aging in primates (4–6). Alzheimer's disease (AD), on the other hand, is characterized by extensive and selective death of neurons and deterioration of synapses and circuits in the brain. AD is the most common form of dementia in the elderly, affecting an estimated 5.7 million Americans in 2018 (3), and this prevalence is expected to increase further in the coming decades.

Nonhuman primates (NHPs), like humans, are vulnerable to age-related cognitive decline and synaptic impairment in the absence of neuronal loss. It does not appear to be the case that NHPs develop tau-based AD pathology reflective of extensive neuron death and massive circuit disruption as human patients with AD do (7), although as reported in this issue of PNAS, very old NHPs can develop tau-based pathologic profiles similar to those in patients with AD. The dorsolateral prefrontal cortex (DLPFC) and

hippocampus are key regions involved in cognitive functions and are especially vulnerable to aging and AD (8, 9). Cognitive functions dependent on the DLPFC are particularly vulnerable to aging, including executive functions, working memory, and goal-directed behavior (10, 11). Our group and others (4, 11–13) have shown that there is a significant decrease in synapse density in area 46 of the DLPFC in aged monkeys, and this is accounted for primarily by the loss of spines on layer 3 pyramidal neurons, the major source of ipsilateral corticocortical circuits and a key class of neurons subserving working memory (14). Generally, dendritic spines can be divided into 3 major categories: mushroom, thin, and stubby (15, 16). Mushroom spines, which have large spine heads, strong AMPA receptor-mediated currents, and perforated synapses, are thought to mediate strong, stable circuits. Thin spines have small nonperforated synapses with an abundance of NMDA receptors and are known to be highly plastic in comparison to the mushroom spines (17, 18). The rapid response of thin spines to changes in synaptic activity led to the suggestion that they are associated with learning processes, whereas the stability of the mushroom spines suggests their association with long-term memories and strongly embedded circuit attributes such as expertise (19). Nearly half (46%) of thin spines on layer 3 pyramidal neurons in area 46 are lost with aging in rhesus monkeys, whereas there is no loss of mushroom or stubby spines with age. We have also shown that presynaptic mitochondrial morphology reflective of pathology may contribute to synaptic and cognitive aging in area 46 (20), as well as synaptic redistribution of NMDA receptors (21), both of which are modulated by estrogen treatment (22). Importantly, synaptic vulnerability with aging differs fundamentally between area 46 and the dentate gyrus (DG) within the hippocampus, the major recipient of input from the entorhinal cortex. The classes of excitatory synapses that are vulnerable in dentate gyrus include perforated synapses, which in contrast to the thin spines of area 46 are notable for their synaptic stability, strength, and high

This paper results from the Arthur M. Sackler Colloquium of the National Academy of Sciences, "Using Monkey Models to Understand and Develop Treatments for Human Brain Disorders," held January 7–8, 2019, at the Arnold and Mabel Beckman Center of the National Academies of Sciences and Engineering in Irvine, CA. NAS colloquia began in 1991 and have been published in PNAS since 1995. From February 2001 through May 2019 colloquia were supported by a generous gift from The Dame Jillian and Dr. Arthur M. Sackler Foundation for the Arts, Sciences, & Humanities, in memory of Dame Sackler's husband, Arthur M. Sackler. The complete program and video recordings of most presentations are available on the NAS website at <http://www.nasonline.org/using-monkey-models>.

Author contributions: D.B., E.B.-M., P.H.R., M.G.B., and J.H.M. designed research; D.B., S.O., K.D.-C., W.G.J., E.B.-M., and P.H.R. performed research; D.B. and J.H.M. analyzed data; and D.B., M.G.B., and J.H.M. wrote the paper.

The authors declare no conflict of interest.

This article is a PNAS Direct Submission. E.A.B. is a guest editor invited by the Editorial Board.

Published under the PNAS license.

<sup>1</sup>To whom correspondence may be addressed. Email: [jhmorrison@ucdavis.edu](mailto:jhmorrison@ucdavis.edu).

This article contains supporting information online at <https://www.pnas.org/lookup/suppl/doi:10.1073/pnas.1902301116/-DCSupplemental>.

First published December 23, 2019.

representation of AMPA receptors. There is an age-related alteration in synaptic distribution of AMPA receptors in perforated synapses that correlates with compromised hippocampal mediation of memory in rhesus monkeys (23). Thus, while the pattern of synaptic aging differs across these 2 key regions, these and related findings indicate the presence of certain synaptic changes that are region specific yet compromise synaptic and cognitive health in the absence of frank pathology associated with AD or other neurodegenerative diseases. Nevertheless, these synaptic changes may set the stage for vulnerability to neurodegenerative disease, although such a clear mechanistic progression has not been demonstrated definitively.

In addition to synaptic changes with aging, the development of senescent phenotypes in glia may contribute to age-related vulnerability to neurodegenerative pathology. The development of a senescence phenotype includes cessation of division, suppression of important intracellular pathways, and release of inflammatory signaling molecules and protease enzymes. In neurodegenerative diseases like AD, intrinsic and extrinsic factors stimulate the conversion of normal cells into senescent cells (24). In elderly people, systemic inflammatory diseases can lead to a chronic low-grade inflammatory state in the brain that affects glial cells, including microglia and astrocytes, that are often the first responders to stressful events in the brain (25). These cells start to display a higher production of proinflammatory cytokines and reduce the phagocytosis of molecules like amyloid beta (A $\beta$ ), contributing to cognitive impairment and memory loss (24). Senescent glial cells have an important role in the initiation of AD pathology, and clearance of these cells is able to slow down the disease progression (26). Thus, changes in glia may be important factors in the relationship of aging to neurodegenerative diseases.

The pathogenesis of AD has long been linked to fibrils of A $\beta$  protein that accumulate markedly in AD brains, forming insoluble amyloid plaques; however, during the past decade much of the focus has turned to biologically active soluble oligomers of the A $\beta$  peptide (A $\beta$ Os). These oligomers are potent synaptotoxins, known to accumulate in AD brains and in animal models of the disease (27, 28). Soluble A $\beta$ Os, rather than insoluble fibrils or plaques, trigger synapse failure, now regarded by many as the earliest reflection of AD (27, 29). Synaptic failure has been extensively described in patients and in mouse models of AD. There are several transgenic AD models for studying the pathogenesis of the disease, but their translational impact has been limited. Transgenic AD mouse models carry mutations that are associated with early-onset familial forms of AD, which account for less than 5% of the cases of AD. The vast majority of AD cases are sporadic, with a poorly understood etiology that leads to accumulation and impaired clearance of A $\beta$ O species in the absence of known genetic lesions (27). Another important factor is that most AD studies rely on the use of male animals, although nearly two-thirds of current AD cases are women (30) and after the age of 65 y, the lifetime risk of AD is 1 in 6 for women, whereas it is 1 in 11 for men (31).

We report here the development of an NHP model focused on adult females that may model the earliest phase of AD pathogenesis. Rhesus monkeys were injected with A $\beta$ Os in the lateral ventricle, in a protocol previously described (32), or with A $\beta$  scrambled peptide that reportedly exerts minimal cytotoxicity (33). We evaluated synaptic attributes, neuronal and microglial morphology, and cerebrospinal fluid (CSF) biomarkers of AD. Our data suggest that exogenous administration of A $\beta$ Os in adult female rhesus monkeys results in synaptic dysfunction and neuroinflammation that recapitulate features of age-related synaptic alterations and possibly preclinical AD. This is potentially important because synaptic dysfunction may precede frank neuron death and the onset of dementia by several years and is a far more tractable target for intervention than the degenerative cascade that prevails in the human AD brain (34). In fact, we have demonstrated that age-related synaptic alterations that compromise cognition can be rescued in both rat hippocampus and monkey DLPFC by pharmacologic regulation of glutamate transport (35) and estradiol treatment, respectively

(36). Thus, it is our contention that preserving synaptic health is likely to be the most successful strategy to postpone or prevent the onset of AD.

## Results

**Selective Vulnerability of Cortical Circuits Is Induced by Aging or by Oligomeric A $\beta$  in the Monkey Brain.** In the current work, rhesus monkeys were injected in the lateral ventricle of the brain with 100  $\mu$ g of A $\beta$ Os once per day every 3 d for 24 d, totaling 8 injections, in a protocol previously described by Forny-Germano et al. (32). Additionally, another group of animals were injected with A $\beta$  scrambled peptide that reportedly exerts minimal cytotoxicity (33). The animals were perfused 6 d after the last injection, allowing a very short window of time in which the brain was exposed to A $\beta$ Os. CSF was collected from the animals before the beginning of the experiments, twice during the injections, and right before the injection protocol. The last CSF collection was done right before perfusion (detailed timeline of experiments can be found in *SI Appendix, Fig. S1*). Importantly, due to methodological differences in the monkey surgeries, we were able to ensure that a concentration of 100  $\mu$ g of A $\beta$ Os was injected in the lateral ventricle of the brains in each injection and not an estimated range of 10 to 100  $\mu$ g of A $\beta$ Os as reported by Forny-Germano et al. (32).

We observed that A $\beta$ Os deposit with high affinity in pyramidal neurons of the DLPFC in monkeys, mostly colocalizing with postsynaptic density protein 95 (PSD95) and, to a lesser degree, with the presynaptic marker synaptophysin (Fig. 1*A–E*). Pyramidal neurons were identified in layer III of the DLPFC using an antibody against nonphosphorylated neurofilament protein (NPNFP). Pyramidal cells with a high content of NPNFP are highly vulnerable to AD pathology in humans, likely to develop neurofibrillary tangles (NFTs) (37), and their demise is strongly correlated with the severity of dementia. To further analyze the interaction of A $\beta$ Os with synaptic markers in the DLPFC, we exported the confocal data obtained to Imaris software (Bitplane) and created a surface-rendered 3D neuronal reconstruction isolating only PSD95, synaptophysin, and A $\beta$ O puncta within 2  $\mu$ m of labeled dendritic shafts, as shown in Fig. 1*F*. We were able to visualize and analyze A $\beta$ Os in association with PSD95 (Fig. 1*G*) or with synaptophysin (Fig. 1*H*), presumably associated with the designated dendritic shaft. Quantification of 30 apical segments (6 neurons, 5 segments per neuron) shows A $\beta$ O preferentially binds to PSD95 in comparison with the presynaptic marker synaptophysin (Fig. 1*I*). These findings highlight both the effect of A $\beta$ Os rather than plaques as synaptotoxins and the selective targeting of spines rather than terminals.

We did not perform a similar quantification in the scrambled-A $\beta$ -injected monkeys, given that the control animals lack detectable A $\beta$ Os with an antibody that recognizes only a generic epitope common in oligomers but not in other A $\beta$  species, including fibrils, monomers, or natively folded precursor proteins (38). *SI Appendix, Fig. S2* shows that NPNFP pyramidal cells in layer III of the DLPFC from scrambled-A $\beta$ -injected animals present normal distribution of synaptic markers, but lack A $\beta$ O staining proximal to dendrites.

Area 46 of the DLPFC of NHPs is highly vulnerable to aging (17, 22), which highlights the importance of the rhesus monkey for studying the neurobiological bases of cognitive decline in aging, given that mice and rats do not possess a cortical region directly homologous to primate area 46 (39, 40). Synaptic density of these pyramidal neurons in the DLPFC is substantially reduced in aged monkeys in comparison to young ones (Fig. 2*A* and *B*), and this reduction is reflected in selective loss of highly plastic thin spines, but not stable mushroom spines (Fig. 2*C*). This is reflected by an increase in the average spine head diameter (Fig. 2*D*).

We now show that repeated A $\beta$ O injection in the lateral ventricle of monkeys targets neurons in DLPFC, inducing a prominent reduction in spine density in the A $\beta$ O-injected monkeys relative to scrambled A $\beta$ -peptide-injected or noninjected controls (Fig. 2*E–G*). A significant decrease in the total number of spines was observed in apical and basal dendrites (Fig. 2*H* and *SI*



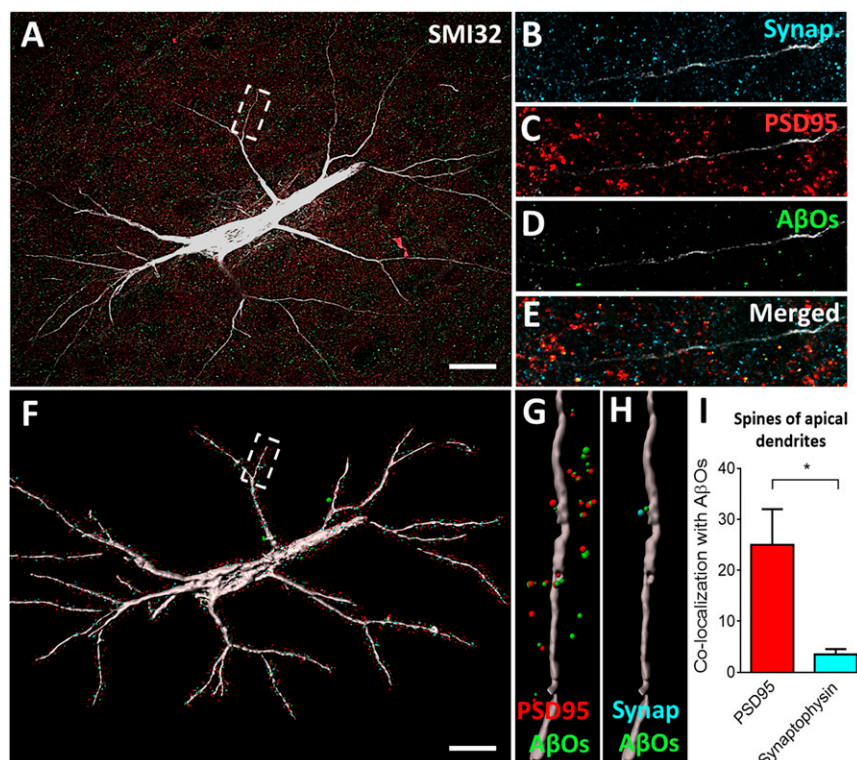


**Fig. 1.** Oligomeric A $\beta$  associates mostly with postsynaptic densities in the DLPFC. (A) Representative projected z stack of a layer III pyramidal neuron stained with SMI32 (white), synaptophysin (blue), PSD95 (red), and A $\beta$ Os (green). An apical segment of this neuron is represented in B–E. (F) The 3D reconstruction of the same neuron maintaining only the puncta staining in a 2- $\mu$ m distance from the neuron. (G and H) Colocalization of PSD95 and A $\beta$ Os (G) and synaptophysin and A $\beta$ Os (H) within a 2- $\mu$ m distance from the neuron. (I) Quantification of colocalization puncta within a 2- $\mu$ m distance from apical segments shows A $\beta$ Os mainly binding to postsynaptic densities in the DLPFC of rhesus monkey. \* $P < 0.05$ , 1-sample t test. (Scale bars: 10  $\mu$ m.)

Appendix, Fig. S3D), driven exclusively by the loss of thin spines. As with aged animals, average spine head diameter was also increased in the A $\beta$ O-injected animals, consistent with the loss of thin spines (Fig. 2I).

Analysis of dendritic branching of pyramidal neurons in layer III of area 46 in the DLPFC showed no effect of A $\beta$ O injection on total dendritic length of the neurons (SI Appendix, Fig. S3E). This mirrors the lack of reduction in overall dendritic arborization with age (17). It is important to note that the differences in spine density between monkeys injected with A $\beta$ Os vs. scrambled A $\beta$  peptide are due to the different composition of the A $\beta$  species. Although both A $\beta$  solutions were prepared freshly before every injection using the same protocol, scrambled A $\beta$  peptides do not oligomerize. Instead, they formed small molecules (monomers) with an average size of 1.8 nm. In comparison, A $\beta$ O particles had an average particle diameter of 4.14 nm, corresponding to oligomers (SI Appendix, Fig. S3F).

Several lines of evidence indicate that deregulation of excitatory transmission can underlie the beginning of synaptic failure in AD. The thin spines are NMDA receptor (NMDAR) dominated (19) and this class of receptor apparently is highly vulnerable to the toxic effects of A $\beta$ Os (41). PSD95 is a major scaffold protein that is enriched with glutamatergic receptors and regulates structural and functional integrity of excitatory synapses. A $\beta$ Os associate with PSD95 in a mechanism that might be dependent on the presence of postsynaptic prion protein and individual glutamate receptors, mainly mGluR5 (42, 43). Further evidence suggests signaling by the complex A $\beta$ O-PrP<sup>C</sup> activates mGluR5 to disrupt neuronal function and induce spine loss (44). Importantly, A $\beta$ Os are present inside synapses in pre- and postsynaptic elements, although more prevalent in excitatory synapses, consistent with a synaptotoxic effect (29).

**Oligomeric A $\beta$  Triggers Microglial Engulfment of Cortical Synapses and Induces Neuroinflammation in the Hippocampus.** Age-related changes in microglia have been characterized by several groups over the last 2 decades (45, 46). These extremely dynamic cells can account for up to 16% of the cells in the human brain (47) and undergo a senescence process that can impair their function and

the interactions with neurons. In normal aging, there is an increase in expression of several inflammatory markers resulting in microglia that are constantly in a primed state, with an activated immune profile (48). Primed microglia are more susceptible to secondary inflammatory stimuli that can trigger an exaggerated inflammatory response, resulting in morphological changes and an activated state (49). Healthy microglia generally present extended and ramified processes, whereas activated microglia display an increase in the size of the cell body and retraction of the branches.

Recently our group demonstrated that aging profoundly affects microglia morphology, and microglia density negatively correlates with spine density of layer III pyramidal cells in the rat medial prefrontal cortex (50). We observed a similar increase in microglia volume in our rhesus monkeys exposed to A $\beta$ Os (Fig. 3A–C), recapitulating the microglial senescence seen in aged rats. Glial cell activation and neuroinflammation also accompany AD pathology and contribute to the development of the disease. Microglia can be activated by the presence of A $\beta$  species and this activation can be harmful to neurons, mediating synapse loss by engulfment of synapses, activating neurotoxic astrocytes, and secreting inflammatory cytokines (51). To investigate a possible role of microglia in the synaptic impairment we observed in the DLPFC, we analyzed microglia morphology and function in our A $\beta$ O-injected and A $\beta$ -scrambled-injected monkeys. Microglia total volume increased in the A $\beta$ O-injected monkeys, in comparison with the A $\beta$ -scrambled-injected and noninjected controls (Fig. 3H). To analyze microglia engulfment of synaptic markers, we applied a similar protocol to that described before (52). Representative 3D reconstruction and surface rendering using Imaris software on DLPFC layer III synapses demonstrate active engulfment of synaptic markers by microglia in monkeys injected with A $\beta$ Os, compared to those injected with A $\beta$ -scrambled peptide (Fig. 3D–G). This analysis showed that PSD95-labeled puncta were far more prevalent than synaptophysin or C1q puncta inside the microglia, demonstrating a selective vulnerability to A $\beta$ Os of postsynaptic spines compared to presynaptic terminals (Fig. 3I–K). We also looked at microglial morphology in the DG of the hippocampus of these monkeys. The DG is thought to be among the most vulnerable sites in the early progression of AD

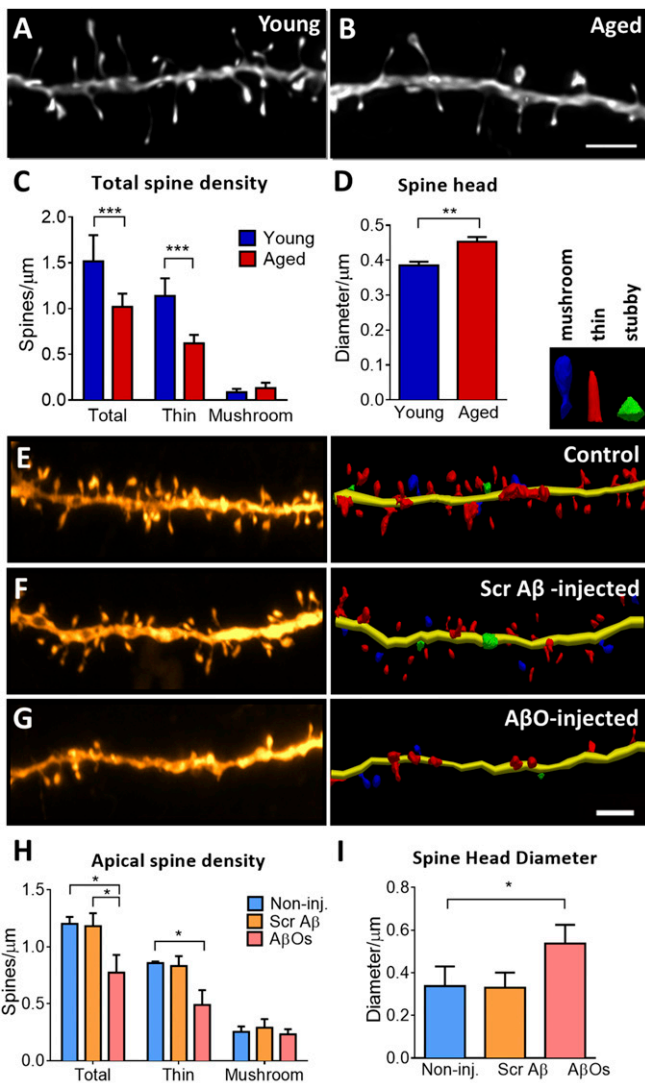


**Fig. 2.** Morphological changes in the DLPFC of rhesus monkey are induced by aging or oligomeric A $\beta$  infusion. (A and B) Representative projected z stacks of a dendrite from a young and an aged animal show a decrease in spine density. (C) Densities of subtypes of spines based on an unbiased classifier show selective loss of thin spines in aging (>22 y old). (D) Average spine head diameter is significantly increased with aging, which is attributable to a selective loss of thin spines. (E–G) Representative projected z stack and 3D neuronal reconstruction of dendritic segments from noninjected control, scrambled A $\beta$ -injected, and A $\beta$ O-injected monkey, showing decrease in spine density. (H) Quantification of apical dendrites shows significant reduction in the total number of spines and in the thin spine density. (I) Average spine head diameter is significantly increased in the apical segments of A $\beta$ O-injected monkey neurons. \* $P < 0.05$ , \*\* $P < 0.01$ , \*\*\* $P < 0.001$ ; 2-sample  $t$  test (spine head diameter young  $\times$  aged), 1-way ANOVA (spine head diameter CTR  $\times$  SCR A $\beta$   $\times$  A $\beta$ O) and 2-way ANOVA, Tukey's post hoc test (spine density). (Scale bar: 2  $\mu$ m.) A–C are adapted with permission from ref. 22.

(53). Four types of microglial morphology were observed in DG: a physiological/resting state with abundant ramifications (*SI Appendix, Fig. S4A*), an intermediate state such as those we observed most often in the DLPFC (*SI Appendix, Fig. S4B*), and amoeboid and rounded microglia (*SI Appendix, Fig. S4C and D*, respectively). The last 2 types were considered reactive microglia. The DG of monkeys injected with A $\beta$ O presented a robust microglial reactive population, as determined by staining with the microglial IBA-1 marker, in comparison with noninjected and scrambled A $\beta$ -injected monkeys (*SI Appendix, Fig. S4E–J*). We observed a

significant increase in the cell body area of microglia in DG of A $\beta$ O monkeys (*SI Appendix, Fig. S4K*), as well as a substantial increase in the microglial reactive population (*SI Appendix, Fig. S4L*). Microglia tended to be more numerous and with fewer branches in the DG of monkeys injected with A $\beta$ O, compared to scrambled peptide or noninjected controls (*SI Appendix, Fig. S4M and N*).

**A $\beta$ O Induce Selective Changes in Core Biomarkers for Alzheimer's Disease in the CSF.** CSF is an optimal source for AD biomarkers since it is in direct contact with the extracellular space of the brain and can directly reflect biochemical changes in the living brain. Further, CSF can be monitored in human patients, increasing the translational relevance of such measures in a NHP model. Core biomarkers such as A $\beta$  and tau levels can be used to identify the progress of the pathogenic events in AD as early as 25 y before expected symptoms (27, 54) and are associated with cognitive decline in patients (55). We collected CSF every 10 d during the A $\beta$ O or A $\beta$ -scrambled injection protocol. There was a substantial increase in A $\beta$  oligomer levels in the CSF of A $\beta$ O-injected animals, with proportional accumulation following the days of injection, but not in the scrambled A $\beta$ -infused animals (Fig. 4A), as would be expected based on our infusion protocol. We also observed an increase in A $\beta$ <sub>1–42</sub> levels, but not A $\beta$ <sub>1–40</sub> during injections in A $\beta$ O-treated monkeys (Fig. 4B and C, respectively). This is consistent with the fact that A $\beta$ O was prepared using A $\beta$ <sub>1–42</sub> human peptide.

Neurofilament light (NFL), a structural component of the cytoskeleton of some neurons, is increased in the CSF of patients with AD as a reflection of degeneration of large-caliber axons (56). We observed no differences in NFL levels following the A $\beta$ O or scrambled peptide injections, suggesting no prominent neurodegenerative process in the time frame employed in this model (Fig. 4E).

Levels of the proinflammatory cytokine TNF- $\alpha$  were increased in the CSF of the A $\beta$ O-treated monkeys (Fig. 4E). This results in the CSF correlate with the increase in microglial activation in the DLPFC and hippocampus and a general neuroinflammatory response in the brain. This increase was specific to the A $\beta$ O injections and not the scrambled peptide control, indicating that these changes were related to effects of the A $\beta$ O peptide conformation and not a general consequence of infusion of a foreign protein into the CSF.

No changes in tau phosphorylation at 3 different sites, serine 199, serine 231, and serine 396, were found during the period of injections, nor were total tau protein levels changed (Fig. 4F–I), suggesting that tau-based pathology was not induced over this time frame, consistent with our observed absence of tau-based cellular pathology in this model. Importantly, all core biomarkers evaluated in the rhesus monkey CSF presented equivalent values compared to human baseline CSF levels or proteins (54, 57).

## Discussion

**Oligomeric A $\beta$  Infusion in the Monkey Brain as a Translational Model of the Early Synaptic Phase of AD.** We report here a quantitative analysis of synaptic alterations and neuroinflammation in an initial study developing a nonhuman primate model of early AD. Our data demonstrate that when injected in the lateral ventricle, A $\beta$ O diffuse and accumulate in areas of the monkey brain relevant to higher-order cognition, including the DLPFC and hippocampus, critical areas in AD pathology (58). Neurons in the DLPFC, vulnerable to aging and neurodegenerative diseases (17), showed specific loss of thin dendritic spines, and these effects are reminiscent of the synaptic disruptions we have observed in cognitively impaired aged monkeys without exogenous A $\beta$ O infusions (17), and may model the early synaptic dysfunction in AD. We also report that A $\beta$ O binds preferentially to PSD95, a postsynaptic marker highly expressed in dendritic spines (59), suggesting a marked loss of spines and confirming A $\beta$ O acting as a postsynaptic toxin in the monkey brain.

Layer III pyramidal neurons of the DLPFC are thought to be the cellular basis of working memory and other high executive



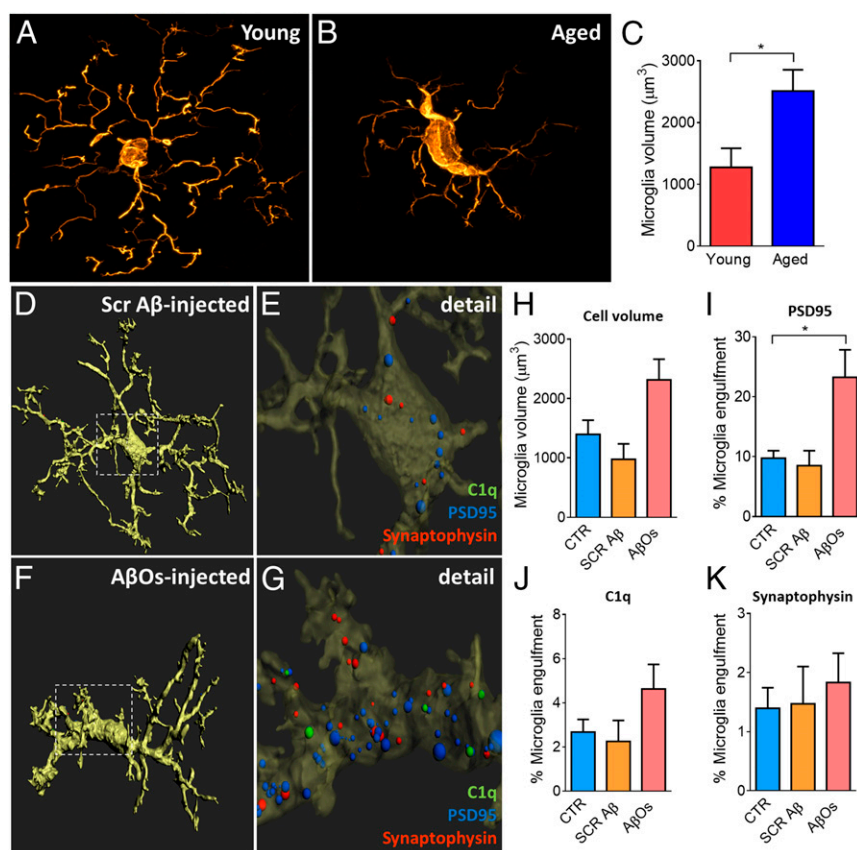


**Fig. 3.** Aging and A $\beta$ O infusion induce morphological changes in microglia. (A–C) Representative images of microglia from a young animal (A) and an aged animal (B) show morphological changes to a more activated state, representing an increase in PFC microglial volume (C). (D–G) Representative surface-rendered microglia from scramble-A $\beta$ -injected and A $\beta$ O-injected animals (D and F), in detail (E and G), with synaptic markers engulfed by microglia, localized mainly in the cell body. (H) Quantification of total volume shows a tendency of increase in the cell body size of A $\beta$ O-injected animals in comparison to noninjected controls and to scrambled-A $\beta$ -injected animals. (I–K) Significant increase of PSD95 puncta inside the microglia of A $\beta$ O-injected animals (I), tendency of increase in C1q complement protein puncta (J), and no differences in synaptophysin puncta (K). \* $P < 0.05$ , 2-sample  $t$  test (microglia volume young  $\times$  aged) or 1-way ANOVA, Tukey's post hoc test (CTR  $\times$  SCR A $\beta$   $\times$  A $\beta$ O). (Scale bar: 5  $\mu\text{m}$ .)

functions (60, 61), and these neurons are enriched with glutamatergic synapses mainly in the thin spines (22, 62), a unique feature of primate evolution highly affected in AD (63, 64). Among the glutamatergic receptors, NMDARs play a pivotal role in the glutamatergic dysfunction observed in AD, interfering with  $\text{Ca}^{2+}$  homeostasis and exacerbating age-related increase of oxidative stress (65). Beta-amyloid can disrupt the balance between synaptic and extrasynaptic NMDAR signaling, reducing glutamatergic transmission and inhibiting synaptic plasticity, likely affecting thin spines on layer III DLPFC pyramidal neurons (66). Tau, on the other hand, normally aggregates in the spine postsynaptic membrane in aged primate DLPFC, which can lead to an early stage of tau pathology that occurs with normal aging (67). The degree to which NMDA-disrupted signaling in layer III DLPFC neurons is caused by A $\beta$ O injections or by normal accumulation of p-tau and correlates with early cognitive dysfunction remains unclear and will be explored in the future.

A $\beta$ O infusions into the monkey brain also induced a distinct pattern of microglial activation in the DLPFC and DG. Normally, microglia in the adult brain surround and support the neurons, facilitating neuronal health and tissue homeostasis in the adult mammalian CNS. In elderly individuals, systemic diseases can trigger microglia priming and induce these cells to acquire a dystrophic stage, which is a sign of microglial cell senescence. In the A $\beta$ O-infused monkeys, we observed similar age-induced dystrophic microglia in the DLPFC. These dystrophic cells have an intense phagocytic activity, engulfing spines, possibly the ones that contain A $\beta$ O bound to postsynaptic markers. Fully reactive microglia devoid of branching processes contain numerous lysosomes and phagosomes. A $\beta$ O-injected monkeys presented an increase in reactive amoeboid and round microglia population in the hilus of the DG in comparison with the control animals, and we did not see similar profiles in the neocortex. Thus, the stage of

activation of microglia in the DG appeared to be more advanced than those in the DLPFC actively phagocytosing spines.

In the CSF, levels of the proinflammatory cytokine TNF- $\alpha$  were increased in A $\beta$ O-injected monkeys following the injections, suggesting an accumulated neuroinflammatory process occurring widespread in the brain. Identification of reliable biomarkers in CSF is extremely useful for early diagnosis and monitoring pathologic progression in AD (68). Analyzing core AD CSF biomarkers, we observed an increase in A $\beta$ 42 and A $\beta$ O levels, but no changes in tau phosphorylation and total tau, suggesting no prominent tau pathology was induced by A $\beta$ O infusion protocol over this time frame. The levels of all AD core biomarkers in the monkey CSF were similar to the levels observed in humans, reinforcing the translational power of the model to recapitulate features of the pathology in humans.

Using high-resolution immunohistochemistry, we also could not detect tau phosphorylation and tangles in different brain regions of A $\beta$ O-injected monkeys, including layer 2 of entorhinal cortex, 1 of the first areas affected during AD pathology progression (SI Appendix, Fig. S5). These results differ from the findings reported by Forny-Germano et al. (32) using the same A $\beta$ O infusion protocol in monkeys, although these authors used cynomolgus monkeys and we used rhesus. There were also differences in the methodology applied across studies, specifically the perfusion protocol and fixation of brain samples. In the current study, at least in the time frame analyzed, development of tangles is not an inevitable consequence of A $\beta$ O-induced synaptotoxicity and neuroinflammation, although longer exposure to A $\beta$ O may induce tau-based pathology.

**A $\beta$ O Accumulation as an Early Event in AD Progression.** New insights into the amyloid hypothesis suggest that rather than amyloid being a singular cause of AD, it more likely functions as an initiator of a complex network of pathological changes, including tau pathology (69). A large body of evidence supports a role for

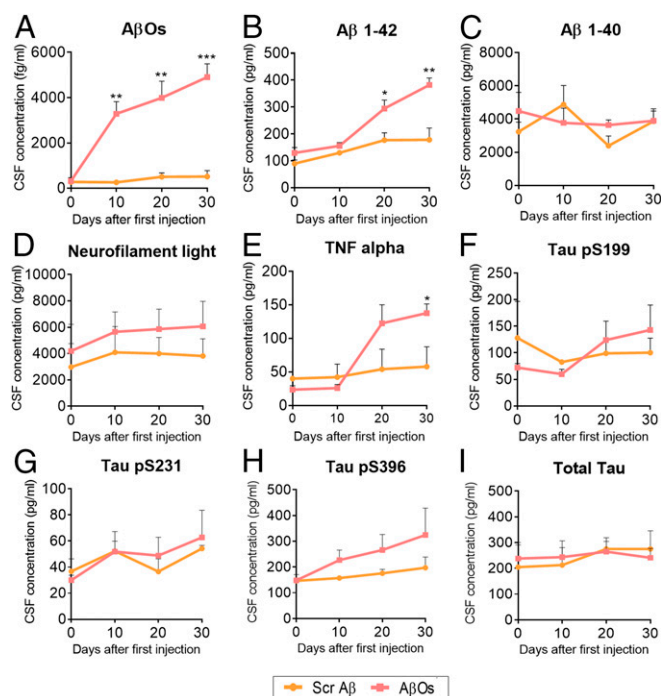


**Fig. 4.** Analysis of AD biomarkers in the CSF of injected animals. CSF was collected every 10 d during the duration of the injections protocol and stored at  $-80^{\circ}\text{C}$  until analysis. (A) A substantial increase in A $\beta$ O levels was observed in A $\beta$ O-injected animals but not in the A $\beta$ -scrambled animals, suggesting the specificity of the preparation injected and that A $\beta$ Os injected in the ventricle spread throughout the brain and reach the CSF. (B and C) A $\beta$ <sub>1-42</sub> (B), but not A $\beta$ <sub>1-40</sub> (C) is increased after A $\beta$ O injections. (D) No changes in neurofilament light were observed. (E) Proinflammatory cytokine TNF- $\alpha$  is increased in the CSF of A $\beta$ O-injected animals, but not in the scrambled A $\beta$  ones. (F–I) No changes in the levels of phospho-tau (p-tau) serine 199 (F), p-tau serine 231 (G), p-tau serine 396 (H), and total tau (I) were observed in both injected animal groups. \* $P < 0.05$ , \*\* $P < 0.01$ , \*\*\* $P < 0.001$ ; 2-way ANOVA, Sidak's post hoc test.

soluble species of A $\beta$  in the synaptic dysfunction likely to dominate the early stages of AD pathologic progression, particularly the oligomeric forms (27, 28). A subtle effect of soluble oligomeric A $\beta$  accumulating and binding to spines can lead to memory loss, beginning early in the disease progression and leading to glia activation, oxidative stress, tau pathology, and widespread neuronal dysfunction (27). The mechanism underlying accumulation of oligomers in sporadic AD is still unknown, but it might involve a drastic reduction in A $\beta$  clearance in AD brains (70).

AD pathological progression likely begins with a “synaptic” phase absent neuron death, followed by a degenerative phase associated with neuron death, and a clinical phase reflecting extensive pathology, with each phase lasting several years (Fig. 5). The synaptic phase involves the earliest events of A $\beta$  oligomerization and binding to spines, inducing the first events of thin spine loss and morphological changes in glial cells. Importantly, our monkey data on normal aging suggest that this phase may stabilize and not progress to the degenerative phase. This likely precedes the accumulation of amyloid plaques and the development of neurofibrillary tangles. From this perspective, for amyloid-based therapies to be successful, they would have to be applied in the synaptic phase, well before the diagnosis of AD or extensive tau pathology.

In the past decades, there has been substantial debate about the validity of the amyloid hypothesis as the dominant model of AD pathogenesis, specifically due to the several failures of clinical trials targeting A $\beta$ . It needs to be noted, however, that most studies targeting anti-amyloid agents were done in patients with dementia clinically apparent, i.e., later in the disease progression when neuron death was likely very extensive. More recently, solanezumab, an antibody against A $\beta$ , did not slow cognitive

decline in patients who had some evidence of amyloid disease detected with an amyloid PET scan (71). This suggests that intervention with anti-amyloid therapy once A $\beta$  deposition in the form of amyloid plaques is detectable, and cognitive decline is present, is also too late to be effective. An ongoing clinical trial, A4 (“anti-amyloid treatment in asymptomatic Alzheimer’s,” NCT02008357), has enrolled more than 1,000 older individuals who have positive amyloid PET scans but do not show cognitive symptoms of AD into a phase 3 double-blind trial of solanezumab vs. placebo. This will provide definitive evidence of whether intervention to disrupt A $\beta$  plaques at this phase of AD pathogenesis is effective. Our model system potentially provides the opportunity to test interventions at an even earlier stage, when A $\beta$ O accumulation has begun and synapses are being targeted, but before formation of A $\beta$  plaques and neuronal loss.

**Do Monkeys Develop Alzheimer’s Disease?** Although mouse models have provided great mechanistic insights into the pathogenesis of AD, we are still in need of additional translationally powerful models, particularly models of sporadic AD, because the current models are generally based on mutations linked to familial AD. The search for a more powerful translational model has led to the use of the NHPs, phylogenetically closer to humans. Macaque monkeys and great apes share 100% homology for the A $\beta$  sequence with humans; great apes share 100% homology and rhesus monkeys 98% homology with humans for the sequence of the longest form of tau protein (72). Gorillas show changes in cytoskeletal tau, but they are distinct from AD-like NFTs (73). The presence of AD-like NFTs was reported recently in a fairly large

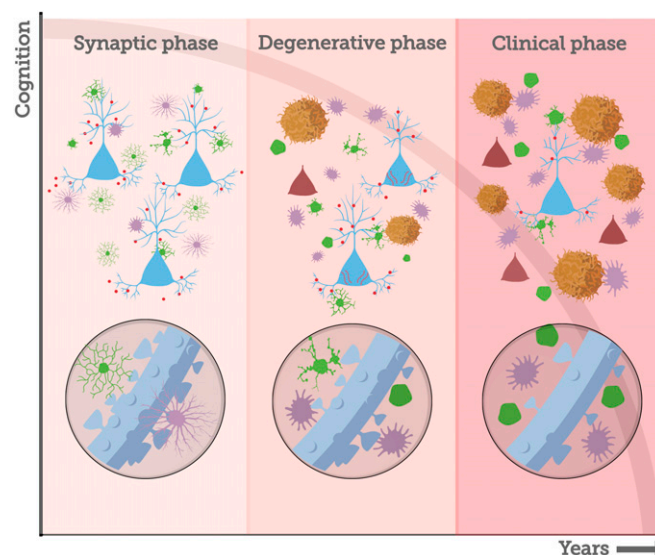


**Fig. 5.** AD pathological temporal progression. Increased A $\beta$ 42 production throughout life (early-onset AD) or failure of A $\beta$  clearance mechanisms (late-onset AD) generates a gradual increase and accumulation of A $\beta$  species in the brain, particularly in the associative cortices (27). A $\beta$  oligomers species (red circles) act as synaptotoxins, binding to dendritic spines and inducing glia morphological changes (green, microglia; purple, astrocyte) and loss of thin spines in the DLPFC. We consider these early events as the synaptic phase of AD, when a very early stage of synaptic disruption can be targeted for interventions that are likely to be effective. Amyloid fibrils and plaques are formed when A $\beta$  oligomers exceed the critical aggregation concentration (81), a process that leads to increase in glial activation and in the neuroinflammatory response. The presence of extracellular A $\beta$  species may trigger the conversion of tau to a toxic state (81), starting the accumulation and spread of neurofibrillary tangles and neuron death, a sequence of events that marks the degenerative phase of AD. Accumulation of soluble toxic aggregates of amyloid and tau, as well as intense tangle and amyloid plaque formation, spreads through different areas of the brain during many years, leading to the clinical phase of the disease, when cognitive impairment and behavioral dysfunction become severe.



group of aged chimpanzees (aged 37 to 62 y) (74), having been shown before only in a single 41-y-old chimpanzee (75). This aligns with the physiological similarity between humans and other hominids, but these observations are from the oldest old animals. Research in chimpanzees has been minimized in most countries, and brain samples are very scarce and not optimal. Also, as others have noted, the cognitive status of these animals was not known (7), so it was not possible to determine whether the presence of apparently pathologic lesions was associated with cognitive decline or dementia.

Paspalas et al. (76) described recently AD-like tau pathology in an aged rhesus monkey, including the presence of NFTs observed using electron microscopy and autophagic vacuoles reflective of neuron death. Others have described the presence of AD-like NFTs in aged African green monkeys (77, 78). These Old World anthropoid species are valuable models for tracking AD-like pathology at the biochemical/histochemical level and suggest that the molecular machinery for NFT formation may exist across primate species. However, human AD requires NFT formation that translates into extensive neuron death and resultant dementia. Thus, confirmation of AD pathology in nonhominids still requires unbiased and detailed stereological quantification to determine whether or not the degree of neuron death is sufficient to model the cognitive aspects of AD, as well as more precise biochemical identification of tau constituents that represent late-stage NFT formation. The transition from age-related cognitive decline, which is clearly evident in NHPs (17), to AD is dependent on the death of specific subpopulations of pyramidal cells in association cortices that furnish long corticocortical projections (79). Although the death of these neurons is related to NFT formation in humans, the transition to dementia requires the loss of a very high number of these neurons, as demonstrated in highly quantitative, stereological studies in human brains linking pretangles, NFTs, neuron counts, and degree of dementia (63, 80). To date, unbiased stereological studies have found no evidence of age-related neuronal loss in hippocampus or entorhinal cortex in macaque monkeys (81, 82), although similar analyses in the oldest old macaques may generate different results. These limitations notwithstanding, the natural occurrence of NFTs in very old monkeys is a key finding and suggests that the biochemical underpinnings of NFT formation are present in the NHP and could be exploited in a model that exacerbates such processes at a younger age. Key advantages and disadvantages of the most common models of AD are highlighted in *SI Appendix, Fig. S6*.

## Conclusion

For many decades, we have been relying on mouse models to provide preclinical data for AD therapeutics, with more than 200 interventions having been reported to ameliorate AD-related pathology in mice, but no successful translation to therapies for humans (83). These models recapitulate better symptomatic phases of AD, but fail to recapitulate the earliest synaptic stages of the disease (84, 85). This study may help address the issue of whether or not targeting soluble A $\beta$ Os early in the process can affect the progression of decline.

Accumulation and oligomerization of A $\beta$  in the brain is thought to begin up to 20 y prior to clinical AD (27). Together with subtle inflammatory responses including microglial activation, A $\beta$ Os lead to early stages of synapse disruption, likely years before notable behavioral decline, metabolic dysfunction, or neuronal loss occurs. Old World monkeys provide an excellent model for studying these early events in the cascade of AD pathology, although it is still not clear whether these animals normally develop neuron death

sufficient to induce dementia. We propose here that adult rhesus monkeys injected with A $\beta$ Os mimic the very early stages of AD pathology in humans, allowing us to understand how A $\beta$  binds preferentially to some neurons but not others and how the first steps of microglial activation could lead to synapse loss and potentially neuron loss. Additional NHP models need to be developed that more aggressively target the degenerative phase, perhaps by directly manipulating tau genetics and biochemistry in live monkeys.

One important next step is to understand how variation in hormones may impact disease progression, since it is clear that estrogen treatment can impact synaptic health in aged rhesus monkeys (36). To that end, the potential role of ovarian hormone replacement in aged females needs to be evaluated further in these models, as this is 1 major concern in women undergoing hormonal changes during menopausal transition.

## Materials and Methods

**Animals.** All experiments were conducted in compliance with the National Institutes of Health Guidelines for the Care and Use of Experimental Animals, approved by the Institutional Animal Care and Use Committee at the University of California, Davis (protocol no. 18994). Nine adult female (age range: 11 to 19 y old) rhesus monkeys (*Macaca mulatta*) and 3 aged female adults (age range: 22 to 28 y old) were used for morphometric analyses and biochemical assays. Four monkeys were injected with A $\beta$ Os, 2 monkeys with scrambled A $\beta$  peptide, and 3 age-matched female animals were used as noninjected controls. Details of monkeys' surgeries, MRI, perfusion, and tissue and CSF collection can be found in *SI Appendix*.

**A $\beta$ Os and Scrambled A $\beta$  Preparation.** Synthetic A $\beta_{1-42}$  human peptide (California Peptide) and Scrambled A $\beta_{1-42}$  peptide (Bachem) were used to prepare A $\beta$  solutions as previously described (86). Scrambled A $\beta_{1-42}$  peptide (Bachem) consists of a peptide with the same amino acid composition, but in random sequence. Please see *SI Appendix* for details about A $\beta$  solution infusions.

**Immunohistochemistry.** Fifty-micrometer-thick free-floating sections were incubated in an antigen retriever solution (Wako; S1700) at 95 °C for 30 min. After that, sections were incubated in blocking solution: 5% donkey serum, 5% goat serum, 5% BSA in PBS, and 0.3% Triton for 2 h at RT under agitation. Sections were then incubated overnight with A11 (code AHB0052, Thermo Fisher; 1:500), SMI32 (code NE1023, EMD Millipore; 1:500), synaptophysin 1 (code 101004, Synaptic Systems; 1:1,000), PSD95 (code ab12093, Abcam; 1:1,000), IBA-1 (code 234-006, Synaptic Systems; 1:1,000), and C1q (code ab182451, Abcam; 1:400) antibodies. Tissue was washed thoroughly with PBS and incubated with Alexa Fluor secondary antibodies (Invitrogen; 1:500) for 2 h, at room temperature. TrueBlack solution (Biotium) was used for 30 min to eliminate lipofuscin autofluorescence. Slides were then mounted with Prolong Diamond Antifade with Dapi (Invitrogen). See *SI Appendix* for microscopy image analysis.

**Statistical Analysis.** All analyses were performed with GraphPad Prism, and datasets were assessed for normality parameters prior to significance determination. Values are expressed as means  $\pm$  SEM, unless otherwise stated. Statistical tests and confidence levels are indicated in Figs. 1–4 (\* $P$  < 0.05, \*\* $P$  < 0.01, \*\*\* $P$  < 0.001). A more detailed table with information about statistical tests performed and the values can be found in *SI Appendix*.

**ACKNOWLEDGMENTS.** We thank Jeffrey Roberts, Mary Roberts, Lisa Novik, Silvia Hilt, John Voss, Anne Gibbons, Sarah Motley, Amanda Dao, Eric Zhou, and Marc Friedmann for expert technical assistance. We also thank Patrick Hof and Lee Way Jin for the human brain samples and Virginia Lee for the kind gift of A $\beta$  oligomer-specific NAB61 antibody. This project was supported by NIH Grants P01-AG016765, R37-AG06647, and P51-OD011107. The California National Primate Research Center is supported by NIH Office of the Director Award P51-OD011107.

1. G. K. Vincent, V. A. Velkoff, Eds., "The next four decades: The older population in the United States: 2010 to 2050" in *Current Population Reports* (US Census Bureau, Washington, DC, 2010), P25-1138.
2. C. N. Harada, M. C. Natelson Love, K. L. Triebel, Normal cognitive aging. *Clin. Geriatr. Med.* **29**, 737–752 (2013).
3. I. Mebane-Sims; Alzheimer's Association, 2018 Alzheimer's disease facts and figures. *Alzheimers Dement.* **14**, 367–429 (2018).
4. A. Peters, D. Leahu, M. B. Moss, K. J. McNally, The effects of aging on area 46 of the frontal cortex of the rhesus monkey. *Cereb. Cortex* **4**, 621–635 (1994).

5. A. Peters, J. H. Morrison, D. L. Rosene, B. T. Hyman, Feature article: Are neurons lost from the primate cerebral cortex during normal aging? *Cereb. Cortex* **8**, 295–300 (1998).
6. A. Peters, C. Sethares, The effects of age on the cells in layer 1 of primate cerebral cortex. *Cereb. Cortex* **12**, 27–36 (2002).
7. L. C. Walker, M. Jucker, The exceptional vulnerability of humans to Alzheimer's disease. *Trends Mol. Med.* **23**, 534–545 (2017).
8. J. H. Morrison, P. R. Hof, Life and death of neurons in the aging cerebral cortex. *Int. Rev. Neurobiol.* **81**, 41–57 (2007).

9. J. H. Morrison, P. R. Hof, Selective vulnerability of corticocortical and hippocampal circuits in aging and Alzheimer's disease. *Prog. Brain Res.* **136**, 467–486 (2002).
10. R. T. Bartus, D. Fleming, H. R. Johnson, Aging in the rhesus monkey: Debilitating effects on short-term memory. *J. Gerontol.* **33**, 858–871 (1978).
11. T. L. Moore, R. J. Killiany, J. G. Herndon, D. L. Rosene, M. B. Moss, Executive system dysfunction occurs as early as middle-age in the rhesus monkey. *Neurobiol. Aging* **27**, 1484–1493 (2006).
12. A. Peters, M. B. Moss, C. Sethares, The effects of aging on layer 1 of primary visual cortex in the rhesus monkey. *Cereb. Cortex* **11**, 93–103 (2001).
13. S. N. Burke et al., Orbitofrontal cortex volume in area 11/13 predicts reward devaluation, but not reversal learning performance, in young and aged monkeys. *J. Neurosci.* **34**, 9905–9916 (2014).
14. M. Wang et al., Neuronal basis of age-related working memory decline. *Nature* **476**, 210–213 (2011).
15. A. Peters, I. R. Kaiserman-Abramof, The small pyramidal neuron of the rat cerebral cortex. The perikaryon, dendrites and spines. *Am. J. Anat.* **127**, 321–355 (1970).
16. K. M. Harris, S. B. Kater, Dendritic spines: Cellular specializations imparting both stability and flexibility to synaptic function. *Annu. Rev. Neurosci.* **17**, 341–371 (1994).
17. J. H. Morrison, M. G. Baxter, The ageing cortical synapse: Hallmarks and implications for cognitive decline. *Nat. Rev. Neurosci.* **13**, 240–250 (2012).
18. J. H. Morrison, M. G. Baxter, Synaptic health. *JAMA Psychiatry* **71**, 835–837 (2014).
19. J. Bourne, K. M. Harris, Do thin spines learn to be mushroom spines that remember? *Curr. Opin. Neurobiol.* **17**, 381–386 (2007).
20. Y. Hara et al., Presynaptic mitochondrial morphology in monkey prefrontal cortex correlates with working memory and is improved with estrogen treatment. *Proc. Natl. Acad. Sci. U.S.A.* **111**, 486–491 (2014).
21. Y. Hara et al., Estrogen alters the synaptic distribution of phospho-GluN2B in the dorsolateral prefrontal cortex while promoting working memory in aged rhesus monkeys. *Neuroscience* **394**, 303–315 (2018).
22. D. Dumitriu et al., Selective changes in thin spine density and morphology in monkey prefrontal cortex correlate with aging-related cognitive impairment. *J. Neurosci.* **30**, 7507–7515 (2010).
23. Y. Hara et al., Synaptic distributions of GluA2 and PKM $\zeta$  in the monkey dentate gyrus and their relationships with aging and memory. *J. Neurosci.* **32**, 7336–7344 (2012).
24. D. J. Baker, R. C. Petersen, Cellular senescence in brain aging and neurodegenerative diseases: Evidence and perspectives. *J. Clin. Invest.* **128**, 1208–1216 (2018).
25. M. Kritsilis et al., Ageing, cellular senescence and neurodegenerative disease. *Int. J. Mol. Sci.* **19**, E2937 (2018).
26. T. J. Bussan et al., Clearance of senescent glial cells prevents tau-dependent pathology and cognitive decline. *Nature* **562**, 578–582 (2018).
27. D. J. Selkoe, J. Hardy, The amyloid hypothesis of Alzheimer's disease at 25 years. *EMBO Mol. Med.* **8**, 595–608 (2016).
28. R. E. Tanzi, The synaptic Abeta hypothesis of Alzheimer disease. *Nat. Neurosci.* **8**, 977–979 (2005).
29. E. K. Pickett et al., Non-fibrillar oligomeric amyloid- $\beta$  within synapses. *J. Alzheimers Dis.* **53**, 787–800 (2016).
30. R. Brookmeyer et al., National estimates of the prevalence of Alzheimer's disease in the United States. *Alzheimers Dement.* **7**, 61–73 (2011).
31. Alzheimer's Association, 2017 Alzheimer's disease facts and figures. *Alzheimers Dement.* **13**, 325–373 (2017).
32. L. Forny-Germano et al., Alzheimer's disease-like pathology induced by amyloid- $\beta$  oligomers in nonhuman primates. *J. Neurosci.* **34**, 13629–13643 (2014).
33. D. M. Vadukul, O. Gbajumo, K. E. Marshall, L. C. Serpell, Amyloidogenicity and toxicity of the reverse and scrambled variants of amyloid- $\beta$  1–42. *FEBS Lett.* **591**, 822–830 (2017).
34. D. M. Holtzman, J. C. Morris, A. M. Goate, Alzheimer's disease: The challenge of the second century. *Sci. Transl. Med.* **3**, 77s1 (2011).
35. A. C. Pereira et al., Glutamatergic regulation prevents hippocampal-dependent age-related cognitive decline through dendritic spine clustering. *Proc. Natl. Acad. Sci. U.S.A.* **111**, 18733–18738 (2014).
36. Y. Hara, E. M. Waters, B. S. McEwen, J. H. Morrison, Estrogen effects on cognitive and synaptic health over the lifespan. *Physiol. Rev.* **95**, 785–807 (2015).
37. P. R. Hof, J. H. Morrison, The aging brain: Morphomolecular senescence of cortical circuits. *Trends Neurosci.* **27**, 607–613 (2004).
38. R. Kaye et al., Fibril specific, conformation dependent antibodies recognize a generic epitope common to amyloid fibrils and fibrillar oligomers that is absent in prefibrillar oligomers. *Mol. Neurodegener.* **2**, 18 (2007).
39. S. P. Wise, Forward frontal fields: Phylogeny and fundamental function. *Trends Neurosci.* **31**, 599–608 (2008).
40. M. Laubach, L. M. Amarante, K. Swanson, S. R. White, What, if anything, is rodent prefrontal cortex? *eNeuro* **5**, ENEURO.0315-18.2018 (2008).
41. G. M. Shankar et al., Natural oligomers of the Alzheimer amyloid-beta protein induce reversible synapse loss by modulating an NMDA-type glutamate receptor-dependent signaling pathway. *J. Neurosci.* **27**, 2866–2875 (2007).
42. M. Renner et al., Deleterious effects of amyloid  $\beta$  oligomers acting as an extracellular scaffold for mGluR5. *Neuron* **66**, 739–754 (2010).
43. J. W. Um et al., Alzheimer amyloid- $\beta$  oligomer bound to postsynaptic prion protein activates Fyn to impair neurons. *Nat. Neurosci.* **15**, 1227–1235 (2012).
44. J. W. Um et al., Metabotropic glutamate receptor 5 is a coreceptor for Alzheimer A $\beta$  oligomer bound to cellular prion protein. *Neuron* **79**, 887–902 (2013).
45. P. L. McGeer, J. Rogers, E. G. McGeer, Inflammation, antiinflammatory agents, and Alzheimer's disease: The last 22 years. *J. Alzheimers Dis.* **54**, 853–857 (2016).
46. B. Spittau, Aging microglia-phenotypes, functions and implications for age-related neurodegenerative diseases. *Front. Aging Neurosci.* **9**, 194 (2017).
47. M. Mittelbronn, K. Dietz, H. J. Schluesener, R. Meyermann, Local distribution of microglia in the normal adult human central nervous system differs by up to one order of magnitude. *Acta Neuropathol.* **101**, 249–255 (2001).
48. D. M. Norden, J. P. Godbout, Review: Microglia of the aged brain: Primed to be activated and resistant to regulation. *Neuropathol. Appl. Neurobiol.* **39**, 19–34 (2013).
49. V. H. Perry, C. Holmes, Microglial priming in neurodegenerative disease. *Nat. Rev. Neurol.* **10**, 217–224 (2014).
50. T. E. Chan et al., Cell-type specific changes in glial morphology and glucocorticoid expression during stress and aging in the medial prefrontal cortex. *Front. Aging Neurosci.* **10**, 146 (2018).
51. M. T. Heneka et al., Neuroinflammation in Alzheimer's disease. *Lancet Neurol.* **14**, 388–405 (2015).
52. D. P. Schafer et al., Microglia sculpt postnatal neural circuits in an activity and complement-dependent manner. *Neuron* **74**, 691–705 (2012).
53. S. A. Small, S. A. Schobel, R. B. Buxton, M. P. Witter, C. A. Barnes, A pathophysiological framework of hippocampal dysfunction in ageing and disease. *Nat. Rev. Neurosci.* **12**, 585–601 (2011).
54. K. Blennow, H. Zetterberg, A. M. Fagan, Fluid biomarkers in Alzheimer disease. *Cold Spring Harb. Perspect. Med.* **2**, a006221 (2012).
55. A. N. Santos et al., Amyloid- $\beta$  oligomers in cerebrospinal fluid are associated with cognitive decline in patients with Alzheimer's disease. *J. Alzheimers Dis.* **29**, 171–176 (2012).
56. H. Zetterberg et al., Alzheimer's Disease Neuroimaging Initiative, Association of cerebrospinal fluid neurofilament light concentration with Alzheimer disease progression. *JAMA Neurol.* **73**, 60–67 (2016).
57. K. Blennow, H. Hampel, M. Weiner, H. Zetterberg, Cerebrospinal fluid and plasma biomarkers in Alzheimer disease. *Nat. Rev. Neurol.* **6**, 131–144 (2010).
58. R. D. Terry et al., Physical basis of cognitive alterations in Alzheimer's disease: Synapse loss is the major correlate of cognitive impairment. *Ann. Neurol.* **30**, 572–580 (1991).
59. X. Chen et al., PSD-95 is required to sustain the molecular organization of the post-synaptic density. *J. Neurosci.* **31**, 6329–6338 (2011).
60. P. S. Goldman-Rakic, Cellular basis of working memory. *Neuron* **14**, 477–485 (1995).
61. G. González-Burgos, G. Barrionuevo, D. A. Lewis, Horizontal synaptic connections in monkey prefrontal cortex: An in vitro electrophysiological study. *Cereb. Cortex* **10**, 82–92 (2000).
62. C. D. Paspalas, M. Wang, A. F. T. Arnsten, Constellation of HCN channels and cAMP regulating proteins in dendritic spines of the primate prefrontal cortex: Potential substrate for working memory deficits in schizophrenia. *Cereb. Cortex* **23**, 1643–1654 (2013).
63. T. Bussière et al., Progressive degeneration of nonphosphorylated neurofilament protein-enriched pyramidal neurons predicts cognitive impairment in Alzheimer's disease: Stereologic analysis of prefrontal cortex area 9. *J. Comp. Neurol.* **463**, 281–302 (2003).
64. G. N. Elston, Cortex, cognition and the cell: New insights into the pyramidal neuron and prefrontal function. *Cereb. Cortex* **13**, 1124–1138 (2003).
65. R. Wang, P. H. Reddy, Role of glutamate and NMDA receptors in Alzheimer's disease. *J. Alzheimers Dis.* **57**, 1041–1048 (2017).
66. E. M. Snyder et al., Regulation of NMDA receptor trafficking by amyloid-beta. *Nat. Neurosci.* **8**, 1051–1058 (2005).
67. B. C. Carlyle et al., cAMP-PKA phosphorylation of tau confers risk for degeneration in aging association cortex. *Proc. Natl. Acad. Sci. U.S.A.* **111**, 5036–5041 (2014).
68. J. L. Molinuevo et al., Current state of Alzheimer's fluid biomarkers. *Acta Neuropathol.* **136**, 821–853 (2018).
69. E. S. Musiek, D. M. Holtzman, Three dimensions of the amyloid hypothesis: Time, space and 'wingmen'. *Nat. Neurosci.* **18**, 800–806 (2015).
70. K. G. Mawuenyega et al., Decreased clearance of CNS beta-amyloid in Alzheimer's disease. *Science* **330**, 1774 (2010).
71. L. S. Honig et al., Trial of solanezumab for mild dementia due to Alzheimer's disease. *N. Engl. J. Med.* **378**, 321–330 (2018).
72. E. Drummond, T. Wisniewski, Alzheimer's disease: Experimental models and reality. *Acta Neuropathol.* **133**, 155–175 (2017).
73. S. E. Perez et al., Early Alzheimer's disease-type pathology in the frontal cortex of wild mountain gorillas (*Gorilla beringei beringei*). *Neurobiol. Aging* **39**, 195–201 (2016).
74. M. K. Edler et al., Aged chimpanzees exhibit pathologic hallmarks of Alzheimer's disease. *Neurobiol. Aging* **59**, 107–120 (2017).
75. R. F. Rosen et al., Tauopathy with paired helical filaments in an aged chimpanzee. *J. Comp. Neurol.* **509**, 259–270 (2008).
76. C. D. Paspalas et al., The aged rhesus macaque manifests Braak stage III/IV Alzheimer's-like pathology. *Alzheimers Dement.* **14**, 680–691 (2018).
77. P. E. Cramer et al., Aging African green monkeys manifest transcriptional, pathological, and cognitive hallmarks of human Alzheimer's disease. *Neurobiol. Aging* **64**, 92–106 (2018).
78. C. S. Latimer et al., A nonhuman primate model of early Alzheimer's disease pathologic change: Implications for disease pathogenesis. *Alzheimers Dement.* **15**, 93–105 (2019).
79. J. H. Morrison, P. R. Hof, Life and death of neurons in the aging brain. *Science* **278**, 412–419 (1997).
80. P. R. Hof et al., Stereologic evidence for persistence of viable neurons in layer II of the entorhinal cortex and the CA1 field in Alzheimer disease. *J. Neuropathol. Exp. Neurol.* **62**, 55–67 (2003).
81. J. I. H. Keuter, P. G. M. Luiten, E. Fuchs, Preservation of hippocampal neuron numbers in aged rhesus monkeys. *Neurobiol. Aging* **24**, 157–165 (2003).
82. A. H. Gazzaley, M. M. Thakker, P. R. Hof, J. H. Morrison, Preserved number of entorhinal cortex layer II neurons in aged macaque monkeys. *Neurobiol. Aging* **18**, 549–553 (1997).
83. K. R. Zahs, K. H. Ashe, 'Too much good news'—Are Alzheimer mouse models trying to tell us how to prevent, not cure, Alzheimer's disease? *Trends Neurosci.* **33**, 381–389 (2010).
84. M. P. Murphy, Amyloid-beta solubility in the treatment of Alzheimer's disease. *N. Engl. J. Med.* **378**, 391–392 (2018).
85. D. Beckman, M. G. Baxter, J. H. Morrison, Future directions in animal models of Alzheimer's disease. *J. Neurosci. Res.* **96**, 1829–1830 (2018).
86. M. P. Lambert et al., Diffusible, nonfibrillar ligands derived from A $\beta$ 1–42 are potent central nervous system neurotoxins. *Proc. Natl. Acad. Sci. U.S.A.* **95**, 6448–6453 (1998).